ChemPhysChem

Research Article
doi.org/10.1002/cphc.202500095

Chemistry Europe
European Chemical Societies Publishing

www.chemphyschem.org

Probing Facet Specific Interaction of 2-Propanol and $CoFe_2O_4$ at Near-Ambient Conditions

Anupam Bera,* Soma Salamon, Heiko Wende, Steffen Franzka, Eckart Hasselbrink, and Stéphane Kenmoe*

The interaction between 2-propanol and low-index facets of cobalt ferrite thin films under near-ambient conditions has been studied using surface-sensitive vibrational sum frequency spectroscopy (vSFS) and ab initio molecular dynamics (AIMD) simulations. The experimental and theoretical findings suggest that 2-propanol undergoes molecular and dissociative adsorption on different facets of $CoFe_2O_4$. Dissociation was found to be more prevalent on the (111) surface than on the (001) surface. Under dry conditions, the active regions on the (111) surface consist of Co^{2+}–O_2–propoxide–Fe^{3+} bridges. In contrast, the Co^{2+} surface atoms are inactive on the (001) surface under dry conditions. The Fe^{3+} surface atoms are the preferred adsorption sites. Molecular water plays a detrimental role because it competitively adsorbs onto the active sites with 2-propanol, inhibiting its decomposition. Moreover, OH groups with a lower concentration promote the formation of 2-propoxide. These results contrast with our recent study in which 2-propanol remained molecularly adsorbed on the Co_3O_4 (001) surface. These findings underscore the ambivalent role of hydroxyl groups on surfaces and also highlight the importance of dissociation state and water concentration as critical parameters for 2-propanol activation.

1. Introduction

The catalytic activity of a crystal may well be highly sensitive to the specific facet present. In the past, numerous studies on heterogeneous catalysis on metal oxides have focused on the control of faceting to optimize the selectivity and efficiency of a catalytic reaction.[1–4] In this regard, a comprehensive understanding of the facet-dependent initial mechanistic steps, including an understanding of the adsorption properties such as composition, structure, and orientation of the adsorbates, is a crucial element. Here, we have investigated the interaction of 2-propanol with different low-index facets of $CoFe_2O_4$ surfaces at near-ambient conditions. The study aims to provide fundamental insights to facilitate the facet-engineering based strategy for the optimal design of metal oxide-based catalysts.

Recently, cobalt-based metal oxides, such as Co_3O_4 and $CoFe_2O_4$, have emerged as a promising class of metal oxide catalysts due to their versatility in structure and composition. The presence of octahedral and tetrahedral sites in both normal and inverse spinels, along with the ability to vary the catalyst composition over a wide range, contribute to the potential of these materials as next-generation catalysts. Among other processes, the heterogeneous oxidation of alcohol species has large industrial relevance.[5,6] Nevertheless, the interaction between 2-propanol and $CoFe_2O_4$ has received marginal attention. In a recent study, Falk et al. investigated the oxidation of 2-propanol over a range of $Co_{1+x}Fe_{2-x}O_4$ spinel oxides in contact with both liquid and gas phases.[7] The findings indicate that an increase in Co content will enhance the catalytic activity of the samples for 2-propanol oxidation. This suggests that the iron-free Co_3O_4 samples exhibit the highest catalytic activity, resulting in the production of acetone as the oxidation product. Furthermore, both XPS and theoretical analysis have suggested that Co^{3+} sites are the active sites for oxidation.[6,9,10] However, in contrast, $CoFe_2O_4$-based surfaces have been observed to produce propene as a dehydration product, in addition to CO_2 at elevated temperatures. This observation indicates that cationic iron species, which are more acidic in nature compared to the cobalt ones, are also present on the catalytically active surface. In addition, in situ diffuse reflectance infrared fourier transform spectroscopy analysis revealed that acetates are the main adsorbates responsible for deactivation, while carbonates are only spectator species at the surface.[8]

In this context, our recent study of 2-propanol adsorption on Co_3O_4(001) surfaces at room temperature and near-ambient

A. Bera
School of Chemistry
University of Hyderabad
Prof. C.R. Rao Road, Hyderabad, Telangana 500046, India
E-mail: anupambera@uohyd.ac.in

S. Salamon, H. Wende
Faculty of Physics and Center for Nanointegration (CENIDE)
University of Duisburg-Essen
D-47057 Duisburg, Germany

S. Franzka
Interdisciplinary Center for Analytics on the Nanoscale (ICAN)
University of Duisburg-Essen
D-47057 Duisburg, Germany

E. Hasselbrink, S. Kenmoe
Faculty of Chemistry
University of Duisburg-Essen
D-45117 Essen, Germany
E-mail: stephane.kenmoe@uni-due.de

E. Hasselbrink
Faculty of Chemistry and Center for Nanointegration (CENIDE)
University of Duisburg-Essen
D-45117 Essen, Germany

Supporting information for this article is available on the WWW under https://doi.org/10.1002/cphc.202500095

pressure has shown that surface hydroxylation plays a key role in surface passivation. 2-propanol does not dissociate at room temperature nor at elevated temperatures up to 450 K.[10] Ab initio molecular dynamics (AIMD) simulations, taking into account the presence of an aqueous solvent, showed that the presence of epitactic hydroxyl groups in the vicinity of Co^{3+} sites as well as in the first solvation shell of the organic solute is decisive for the 2-propanol decomposition and subsequent oxidation to acetone. In another AIMD study for dry conditions, 100% dissociation was observed on the Co_3O_4(111) surface at room temperature, while for the (110) face 2-propanol activation was found to be thermally activated.[9] Still, the understanding of the surface chemistry of 2-propanol on cobalt oxide-based catalysts remains incomplete at the molecular level. In the case of $Co_{1+x}Fe_{2-x}O_4$ spinel oxides, the role of Co and Fe active sites as well as the nature and the influence of surface hydroxylation need to be elucidated. In this context, the study of the interaction of alcohols with different low index facets, including (001), (110), and (111), which have different compositions of Co and Fe sites, would be a first step towards a deeper insight into the above questions.

For the study presented here, room temperature second-order nonlinear vibrational sum frequency spectroscopy (vSFS) was used to investigate the reactivity of 2-propanol (at near-ambient pressure) with the (001) and (111) surfaces of $CoFe_2O_4$. vSFS has been demonstrated to be an effective tool due to its inherent surface selectivity which allows surface spectroscopy under real-world, atmospheric pressure conditions.[10–15] Furthermore, vSFS was combined with AIMD simulations to track the dissociation of 2-propanol to 2-propoxide on both surfaces and to identify the active sites, as well as the underlying surface-assisted mechanisms that facilitate 2-propanol activation. Furthermore, it is noteworthy to mention that, as previously discussed in the earlier reports,[10,12] the presence of surface prehydroxylation is inevitable under ambient conditions. The surface prehydration is characterized by the presence of a broad OH region in the vSF spectra (see Figure S5, Supporting Information). Moreover, to gain insight into the nature and role of OH groups involved in the decomposition process, dry, hydrogenated (H-covered), hydroxylated (partially OH-covered), and wet (H_2O covered) surfaces were considered in the simulations.

2. Results and Discussions

The vSFS theory and experimental procedure are discussed in the supporting information. Briefly, in the vSFS experiment, the frequency of the incident mid-IR laser light is tuned via a vibrational resonance of a molecule at the interface, resulting in an increase in the generated sum frequency intensity. However, sum frequency generation is a coherent phenomenon, and thus an ensemble of molecules must have a net orientation to generate SF light, which allows the technique to discriminate against isotropic bulk phases. We focus here on the CH stretching vibration of 2-propanol. **Figure 1** illustrates the fitted vSFS spectra (using Equation (1), Supporting Information) obtained for $CoFe_2O_4$(001)/$SrTiO_3$(001) after exposure to 50 mbar of 2-propanol at room temperature. The spectra were recorded by utilizing the ppp, ssp, and sps polarization combinations (polarizations of SF, visible, and IR, respectively). The vSF spectrum of 2-propanol in the C-H stretching region was discussed in detail in our earlier studies when investigating its interaction with Co_3O_4, TiO_2, and $SrTiO_3$ surfaces.[10,12–14] The analysis of the vSF spectrum of 2-propanol is inherently complex due to the large number of C—H modes present, which frequently overlap and produce multiple Fermi resonances. The complexity is further increased when different species are present on the surface. However, the use of different polarization combinations, specifically ppp, ssp, and sps, allows for the identification of the adsorbed species on the surface.

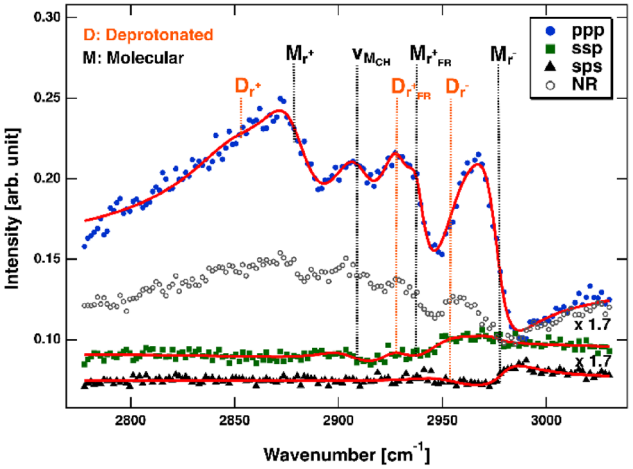

Figure 1. vSF spectra of 2-propanol adsorbed on $CoFe_2O_4$(001)/STO(001) surface obtained with ppp, ssp, and sps polarization combinations (polarizations of SF, visible and IR light, respectively). The ppp spectrum is strongly affected by a nonresonant background. The open gray circles represent the ppp spectrum of the nonresonant (NR) background recorded before exposing the sample to 2-propanol. The solid lines represent fits to the data. The dashed vertical lines indicate the center positions of the identified bands. Features assigned to modes from the intact molecular species are labeled M, and those assigned to the deprotonated species are labeled D.

Our discussion starts with the sps spectrum, in which only for the antisymmetric stretching mode, r^- of CH_3 is active due to symmetry considerations.[1,12–14] The most prominent peak was observed at 2976 cm^{-1} (denoted as M_r^-), which corresponds to the r^- mode of molecular 2-propanol. In addition, a relatively smaller peak was observed at 2950 cm^{-1}. This peak is the characteristic of the deprotonated species (denoted as D_r^-), as evidenced by the shift to lower wavenumbers of the mode. As previously reported, the deprotonated species typically exhibit a shift of all modes to lower wavenumbers by about 20–30 cm^{-1}. Therefore, this observation suggests the coexistence of both molecular and dissociated 2-propanol on the surface at room temperature, but with a higher proportion of molecular 2-propanol. Similarly, two main modes, located at 2880 and 2940 cm^{-1}, are observed in the ssp spectrum: CH_3 symmetric stretching and a Fermi resonance. These are denoted as M_r^+ and $M_r^+{}_{FR}$, respectively, as they originate from molecular 2-propanol. Again, the minor peak at 2925 cm^{-1} is the Fermi resonance from the deprotonated 2-propanol (denoted as $D_r^+{}_{FR}$). However, the most definitive indication of the presence of the dissociated 2-propanol is visible in the ppp spectrum, as it is

the most intense spectrum of all. Four modes appear for molecular 2-propanol, namely the CH_3 symmetric stretching, M_r^+ at 2880 cm^{-1}, ν_{MCH} stretching at 2910 cm^{-1}, a related Fermi resonance with the overtone of the degenerated bending mode ($M_r^+{}_{FR}$) and the antisymmetric mode (M_r^-) at 2940 cm^{-1} and at 2975 cm^{-1}, respectively. The corresponding modes for the deprotonated 2-propanol appear at lower wavenumbers, namely at 2856, 2920, and 2950 cm^{-1}, labeled D_r^+, $D_r^+{}_{FR}$, and D_r^-, respectively. The ν_{DCH} stretching mode of the deprotonated species is most likely hidden between the overlapping M_r+ and $M_r^+{}_{FR}$ modes of the molecular species. Furthermore, it is noteworthy that the lines in the ppp spectrum clearly show dispersive shapes instead of Lorentzian ones due to the presence of a strong nonresonant background, the origin of which was discussed in detail in our previous report.[1,14]

In addition, we estimated the degree of dissociation (using Equation (2), see Supporting Information) by comparing the SF line strengths of the r^+ modes (values are given in the Supporting Information). These are proportional to the number density, assuming that the CH_3 groups of both the deprotonated and molecular species are tilted similarly with respect to the surface normal. The degree of deprotonation is ≈28%.

It is important to note that such dissociation does not occur on the Co_3O_4(001)/MgO(001) surface, as we previously reported.[10] It was concluded that surface prehydroxylation, resulting from the presence of moisture at near-ambient conditions, can reduce surface activity and, consequently, prevent the dissociation of 2-propanol molecules. It is therefore necessary to address the additional role of Fe active sites on surfaces and their influence on O—H bond dissociation. Furthermore, it is important to consider how varying the relative composition of the Fe and Co active sites affects dissociation. The following discussion on the interaction of 2-propanol on $CoFe_2O_4$(111)/$SrTiO_3$(111) provides insight into these. Besides, the role of the elemental composition and spatial distribution of cationic surface sites on the reactivity is discussed below based on the AIMD simulations analyses.

Figure 2 shows the vSFS spectra for $CoFe_2O_4$(111)/$SrTiO_3$(111) after exposure to 50 mbar 2-propanol. In general, the spectral characteristics of the ppp and ssp spectra are comparable to those of the (001) face. In the ppp spectrum, four modes are identified for both molecular and deprotonated 2-propanol. In the case of molecular species, these are as follows: M_r^+ at 2873 cm^{-1}; ν_{MCH} stretching at 2908 cm^{-1}; the Fermi resonance, $M_r^+{}_{FR}$, at 2940 cm^{-1}; and finally, the antisymmetric mode, M_r^-, at 2967 cm^{-1}. For the deprotonated species, the corresponding peaks are observed: D_r^+ at 2856 cm^{-1}; ν_{DCH} at 2896 cm^{-1}; $D_r^+{}_{FR}$ at 2920 cm^{-1}; and D_r^- at 2950 cm^{-1}. The detailed fitting parameters are provided in the supporting information. Note that the ppp spectrum exhibits rather Lorentzian line shapes, indicating that these are not significantly affected by a nonresonant background. Furthermore, it is noteworthy that the sps spectrum exhibits the highest intensity of the three, as can be seen in Figure 2 (The ppp spectrum is multiplied by a factor of 1.5 to allow a better comparison with Figure 1). Additionally, the intense sps spectrum contains the CH_3 symmetric stretching and CH mode, as well as the antisymmetric modes. A further distinction between the (001) and (111) surfaces is the greater extent of

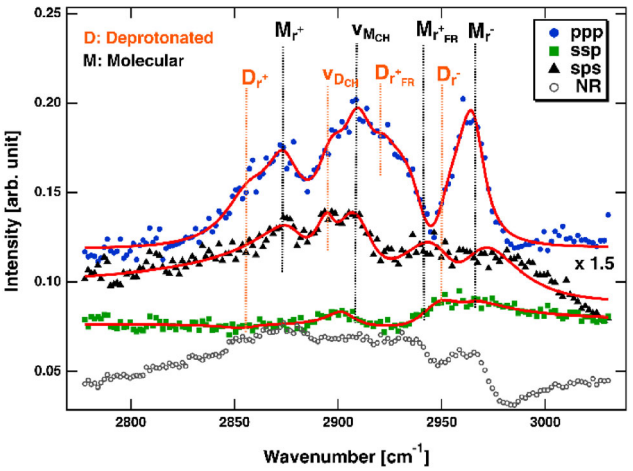

Figure 2. vSF spectra of 2-propanol adsorbed on $CoFe_2O_4$(111)/STO(111) surface obtained with ppp, ssp, and sps polarization combinations (polarizations of SF, visible and IR light, respectively). To achieve better comparability with Figure 1, the ppp spectrum was multiplied by a factor of 1.5. Nevertheless, it should be noted that the sps spectrum displays the highest intensity of the three. The solid lines represent fits to the data. The open gray circles represent the ppp spectrum of the nonresonant (NR) background recorded before exposing the sample to 2-propanol. The dashed vertical lines indicate the center positions of the identified bands. Features assigned to modes from the intact molecular species are labeled M, and those assigned to the deprotonated species are labeled D.

dissociation observed on the latter. The degree of deprotonation is ≈45%, which is higher than that observed on the (001) surface.

However, several key questions remain unanswered. These include investigating the role of Fe, Co, and the reason for the increased deprotonation on the (111) surface. In addition, the role of surface hydroxylation and its influence on the adsorption chemistry requires further investigation. To address these important questions and to provide atomistic insights, we performed AIMD simulations for different $CoFe_2O_4$ facets.

Figure 3 shows snapshots of equilibrium AIMD trajectories at the beginning and the end of the simulations for the $CoFe_2O_4$(111) surface; the one that exposes Co^{2+} in the octahedral sites of the outermost layer and Fe^{3+} in the tetrahedral sites of an adjacent layer, as well as 3-fold (O_1) and 4-fold (O_2) coordinated oxygen atoms. Similar to what was previously observed for the Co_3O_4(111) surface,[9] in dry conditions (S1) the active regions consist of Co^{2+}–$O_{2\text{-propoxide}}$–Fe^{3+} bridges (see Figure 3, top). This is due to the fact that the 3-fold coordinated Fe^{3+} ions occupying the tetrahedral sites are unsaturated and participate in the binding of 2-propanol. Both Co and Fe bind 2-propanol via its oxygen atom. This can be deduced from a comparison of the Co—C and Fe—C bond lengths for which the first maxima in the radial distribution functions (RDF) (**Figure 4** top) are located at 3 and 3.5 Å, respectively, with length of the Co—O and Fe—O bonds. The Co—O bonds with a length centered at 1.9 Å are more prominent while the Fe cations form fewer and weaker bonds with 2-propanol (2.3 Å). Seven out of the eight adsorbed 2-propanol molecules dissociate immediately at the beginning of the simulation ($t \approx 0$ ps) leading to the formation of seven surface OH groups that remain until the end of the simulation. The maximum in the O—H RDF located at 1 Å (Figure 4 bottom) suggests the

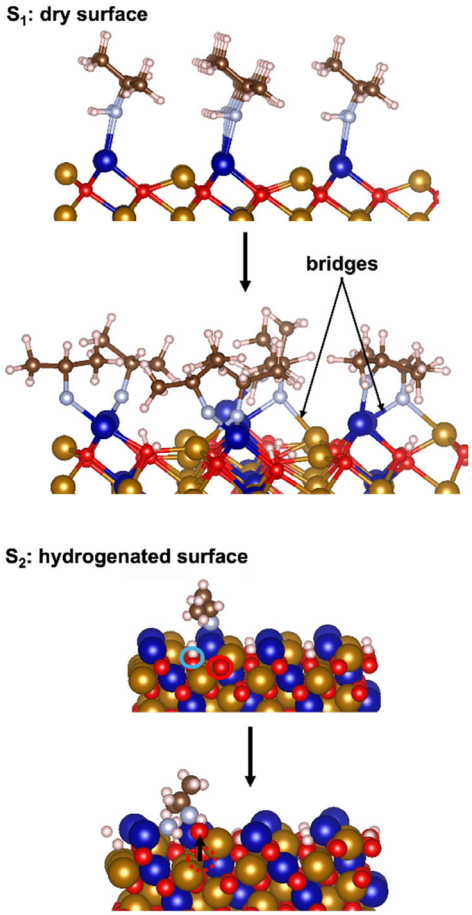

Figure 3. Perspective views of final equilibrium trajectories of 2-propanol on the B-terminated pristine $CoFe_2O_4$(111) surface at 300 K. Top: dry surface at $t = 0$ ps (top) and $t = 20$ ps (bottom). The Co^{2+}–$O_{2\text{-propoxide}}$–Fe^{3+} bridges are indicated; (Bottom): Perspective view of prehydrogenated surface at $t = 0$ ps (top) and $t = 20$ ps (bottom). Co (blue), Fe (brown), O in Co_3O_4 (red), O in 2-propanol (sky-blue), O in water (sky-blue), C (gray), and H (white). Note: that the important sites to watch are highlighted by circles.

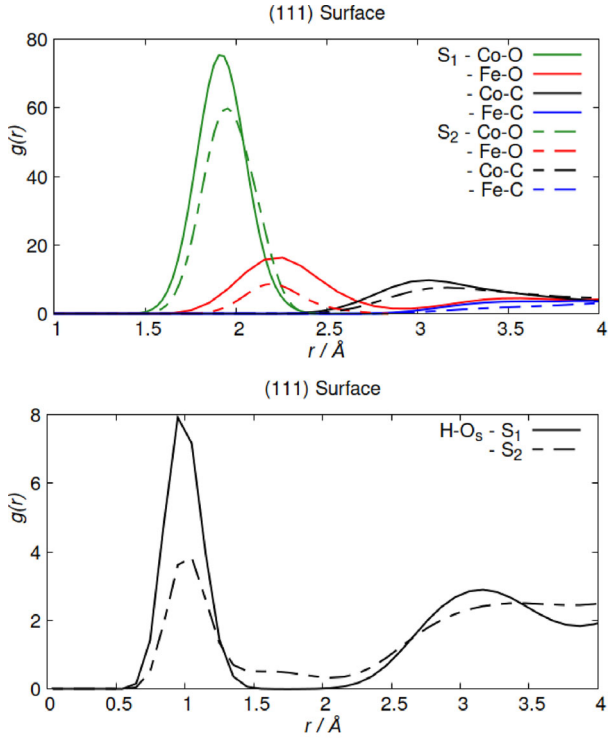

Figure 4. RDF for the dry (S_1) and prehydrogenated (S_2) (111) surfaces. (Top) $g(r_{O\text{-}Co3+})$, $g(r_{O\text{-}Fe3+})$, $g(r_{C\text{-}Co3+})$, and $g(r_{C\text{-}Fe3+})$; (Bottom) $g(r_{H\text{-}Os})$. Here, H and O are the hydrogen and oxygen atoms of the 2-propanol, respectively, and O_s the oxygen atoms in the top surface layer.

presence of surface OH after proton transfer. It can also be deduced from the same figure that the binding mode of 2-propanol consists predominantly of Co—O and Fe—O covalent bonds since H-bonding to the surface is negligible. No recombination was observed. This is because the proton transfer exclusively occurs from the 2-propanol molecule to the unsaturated threefold coordinated surface lattice oxygen atoms (O_1). Unlike the surface oxygen atoms (O_2) located in the outermost oxidic layer which are bound in addition to Co^{2+} and Fe^{3+} located in the top surface layer, these surface oxygen atoms (O_1) only bind to Co^{2+} and Fe^{3+} located in the adjacent metallic sublayer.

In addition, the formation of water was not observed on the clean surface (S_1) during the AIMD simulations. However, evidence for the presence of water was reported during the experimental investigation. This led to the investigation of the adsorption and decomposition of 2-propanol on a hydrogenated surface (S_2), assuming pre-exposure of the surface to water with subsequent formation of surface OH groups. Such a surface was predicted and observed to present the most interesting condition in terms of its relevance to catalysis.[16–18] Figure 3 (bottom) highlights the minute workings of molecular water formation via a Mars–van Krevelen mechanism on a surface where all 3-fold coordinated oxygen atoms (O_1) have been hydrogenated. One of the surface OH groups receives a hydrogen atom upon the deprotonation of a 2-propanol molecule. This results in the formation of a water molecule that immediately desorbs from the surface leaving an oxygen vacancy behind in the top layer of the surface (sky-blue circle). Interfacial OH may be considered as promotive agent for the occurrence of MvK mechanism at low temperature as such a mechanism was also predicted in our recent study on Co_3O_4 surface with the same termination, at the same temperature and under the same H-rich conditions.[9] Also recently, the occurrence of room temperature water-promoted MvK has reported in a joint experimental and computational study of the low-temperature oxidation of CO over Au—Fe_2O_3.[19] Interestingly, one can observe the migration of a lattice oxygen atom from an inner layer to fill the vacancy in the outermost layer (black arrow in red dotted circle, see top left corner of the surface in movie S2 in the supporting information). Such a phenomenon was also reported in a joint experimental and density functional theory study on the anatase TiO_2 (101) surface, which evidenced the stability of oxygen vacancy in the bulk rather than on the surface.[20] The migration of lattice oxygen from the bulk to the surface was found to occur at a lower activation energy (0.75 eV) than the migration into the bulk (1.15 eV).

It should be noted that in the case of the hydrogenated surface S_2, only half of the 2-propanol film dissociates. This is illustrated in Figure 4 (bottom) where one can see the decrease of the

height of the characteristic peak at 1 Å and the formation of relatively strong H-bonds (from 1.5 to 2 Å) between intact 2-propanol molecules and the surface. The water to 2-propanol and water to 2-propoxide ratios are both 1:4 at the end of the simulation. This lower degree of dissociation compared to the clean surface (50 vs. 87.5%) can be explained by the fact that the saturation of 3-fold coordinated O_1 oxygen atoms induces changes in the coordination of oxygen atoms such that they lose their bond to the underlying Fe^{3+} and are thus able to accept transferred protons. As a result of these reconstructions, the Co^{2+}–$O_{2\text{-propoxide}}$–Fe^{3+} bridges are largely broken, leaving the Co sites almost exclusively active and the interaction of 2-propanol with the surface is weakened. This is supported by the narrower overlapping region of the Co—O and Fe—O bonds (1.9 to 2.3 Å vs 1.6 to 2.2 Å in S_1) and the lower amplitudes of the RDFs in Figure 4 (top). However, this degree of dissociation is closer to the experimental value reported above (45%) and may indicate that systems such as S_2 would more closely resemble the experimental conditions.

We have also monitored the adsorption of eight 2-propanol molecules on B-terminated pristine $CoFe_2O_4$(001). This surface exposes both Co^{2+} and Fe^{3+} in the octahedral sites of the topmost layer. **Figure 5** shows snapshots of the initial and final equilibrium trajectories at 300 K for different conditions. In dry conditions (S_3), unlike on the (111) surface, Co^{2+} is inactive. The Fe^{3+} are the preferred adsorption sites, and this holds

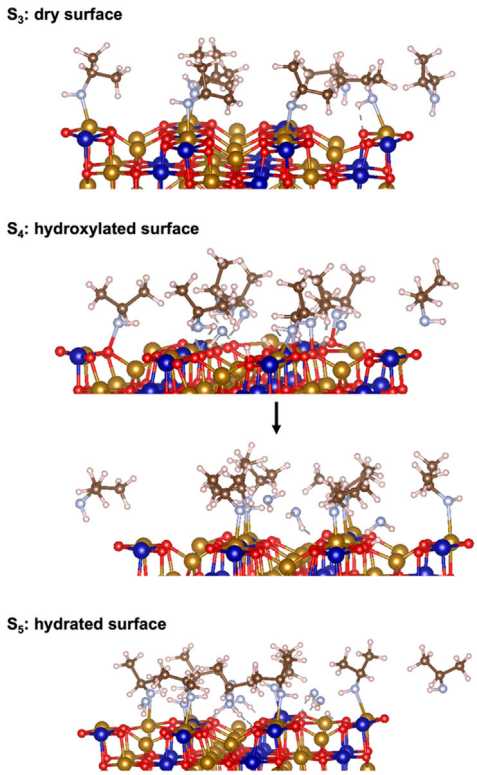

Figure 5. Top and perspective views of final equilibrium trajectories of 2-propanol on the B-terminated pristine $CoFe_2O_4$ (001) surface at 300 K. (Top) dry surface at $t = 15$ ps; (Center): prehydroxylated surface at $t = 0$ ps (top) and $t = 35$ ps (bottom). (Bottom) prehydrated surface at $t = 15$ ps; Co (blue), Fe (brown), O in Co_3O_4 (red), O in 2-propanol (sky-blue), O in water (sky-blue), C (gray), and H (white).

throughout the simulation. In **Figure 6** (Top), the first RDF maxima for the Fe—O and Co—O bonds are located at 2.3 and 3.8 Å, respectively. This supports the formation of strong Fe^{3+}—O bonds and corroborates the sole presence of Fe^{3+} in the contact layer with 2-propanol. None of the eight 2-propanol molecules dissociate and they all remain molecularly adsorbed on top of Fe^{3+} sites during the 20 ps simulation time. As can be seen from Figure 6 (Bottom, left) which shows the RDF of 2-propanol's hydrogen and surface oxygen atoms, there are only H bonds present between the 2-propanol molecules and surface oxygen atoms.

This lower activity of this surface compared to the (111) surface despite the presence of 3-fold undercoordinated oxygens on the surface was also observed for the Co_3O_4(001) surface.[10] Meanwhile, the presence of OH groups in the vicinity of the active sites was found to promote the activation of 2-propanol.[21,22] This motivated us to investigate the impact of interfacial water coverage and its competition with 2-propanol in populating the active sites on $CoFe_2O_4$(001). Therefore, in addition to S_3, we considered another scenario. A hydroxylated surface with preadsorbed water hydroxyls and surface OH resulting from proton transfer to the surface prior to the adsorption of 2-propanol (S_4). In our previous study investigating the adsorption of water on the B-terminated $CoFe_2O_4$(001) surface, it was found that 3 dissociated water molecules can be stabilized on the surface at room temperature together with molecular water in larger proportions.[23] So, the configuration with only the 3 dissociated water molecules remaining on the surface, which could correspond to the surface after exposure to water, was considered in scenario S_4. In order to investigate the effect of a water coverage on the surface reactivity, a hydrated surface with monolayer coverage was also studied (S_5).

Figure 5 (center) shows the effect of OH groups on the reactivity of 2-propanol with the (001) surface (S_4). The OH groups are promoting the activation of 2-propanol and leading to the dissociation of one of the eight molecules on the surface, subsequently followed by formation of molecular water at the interface. The corresponding water to 2-propanol ratio is 1:8 or a dissociation ratio of 12.5%. The formation and coexistence of molecular water with propanol and 2-propoxide is illustrated in Figure 6 (top), where a smaller amplitude peak centered at 2.2 Å exteriorizes the presence of molecular water in addition to OH groups. Interestingly, as with 2-propanol and 2-propoxide—and as also previously reported in Ref. [23]—water competes with the organic adsorbates and occupies exclusively the Fe^{3+} sites throughout the simulation. Upon dissociation of 2-propanol and formation of molecular water, the Fe^{3+}—O bond of the corresponding molecule is shortened as evidenced by the appearance of a shoulder in the first shell seen in the RDF. As supported by Figure 6 (Bottom, left), the formation of 2-propoxide is not assisted by the surface as no proton is transferred to the surface. Only the adjacent OH group facilitates the deprotonation of 2-propanol and no further decomposition of 2-propoxide or recombination of OH groups with surface H was observed during the 35 ps spanned by the simulation. It is important to note that a relatively higher degree of dissociation

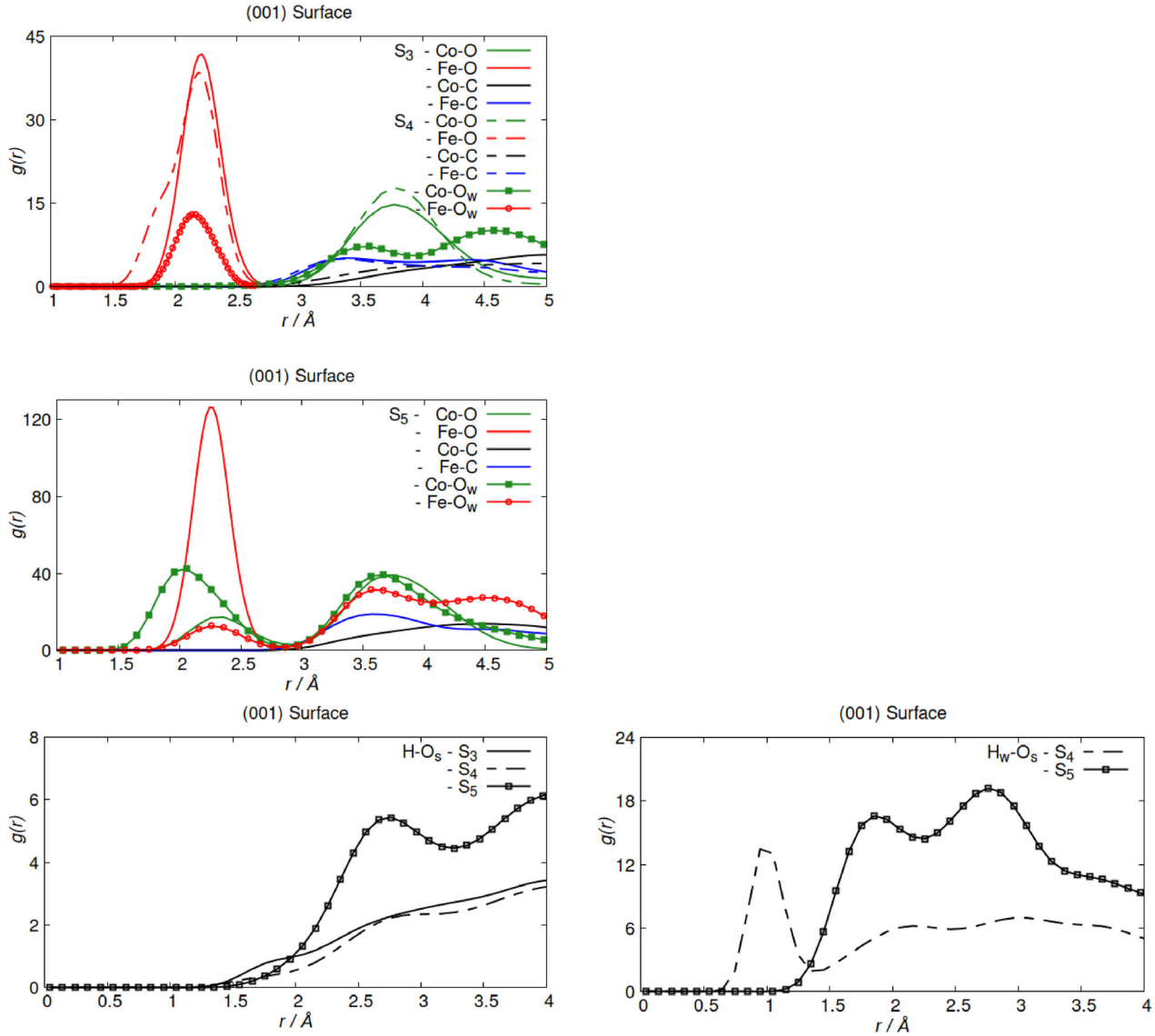

Figure 6. RDFs for the dry (S_3) and prehydrated (S_4) and prehydroxylated (001) surfaces. (Top) $g(r_{O\text{-}Co3+})$, $g(r_{O\text{-}Fe3+})$, $g(r_{C\text{-}Co3+})$ and $g(r_{C\text{-}Fe3+})$; (Bottom, left) $g(r_{H\text{-}Os})$; (Bottom, right) $g(r_{Hw\text{-}Os})$. Here, H and O are the hydrogen and oxygen atoms of 2-propanol, respectively; H_w and O_w are the hydrogen and oxygen atoms of water and O_s the oxygen atoms in the top surface layer.

of 2-propanol was observed in the experiment (≈28%). Longer AIMD trajectories may, however, find a comparable value.

When the water coverage is increased to a monolayer with a 1:1 water to 2-propanol ratio (S_5), both water and 2-propanol molecules occupy Co^{2+} sites in addition to the Fe^{3+} sites, as can be seen from Figure 5 (bottom) and Figure 6 (center). A dissociation ratio of 19% was found in the contact layer with water on this surface.[23] Here, the presence of 2-propanol hinders the dissociation of water. Both water and 2-propanol adsorb molecularly and form additional H-bonds with surface oxygen atoms as can be seen in Figure 6 (Bottom). In contrast to Fe^{3+} sites, water molecules can bind strongly to Co^{2+} sites. This is indicated by the shifts of the Co-Ow bond lengths to smaller values when compared to their Fe-Ow counterparts. Molecular water plays a detrimental role as it can compete for the occupation of active sites with organic solutes and inhibit their decomposition. The state of dissociation and the vapor pressure of water are key parameters for the activation of 2-propanol. This supports the importance of water pretreatment in order to free the surface from molecular water and keep an adequate number of hydroxyl adsorbates that would promote alcohol decomposition.

3. Conclusion

This work presents a unique approach, combining surface-sensitive vSF spectroscopy and AIMD simulation, to study the face-dependent reactivity and selectivity of heterogeneous alcohol dissociation on $CoFe_2O_4$. Most notably, this approach examines the influence of surface pre-exposure to water and subsequent OH group formation on alcohol dissociation under near-ambient conditions. The experimental vSFS results demonstrate the presence of

both molecular and dissociated 2-propanol on both the (111) and (001) surface, with a higher degree of dissociation observed on the (111) surface relative to the (001) counterpart. The AIMD simulation provides atomistic insights into the underlying molecular mechanisms that give rise to these observations. The prehydroxylation of the surface results in a reduction in the extent of dissociation of 2-propanol on the (111) surface compared to the dry surfaces, from 87.5% to 50%. This could be due to the possibility of 2- or 3-fold occupation of cationic sites by water as reported in a recent work,[10,24] or the saturation of active threefold coordinated surface oxygen atoms by hydroxyl and further molecular water formation, following the Mars–van Krevelen mechanism. However, the (001) surface gives contrasting results, as 2-propanol does not dissociate at all on dry surfaces, whereas 2-propanol dissociates after surface hydroxylation, that is, after pre-exposure to water. This observation is attributed to the surface hydroxyl group acting as an oxidizing agent. Furthermore, the presence of both molecularly and dissociatively adsorbed 2-propanol on $CoFe_2O_4$ facets differs from the results of our recent study, where, in the presence of fewer hydroxyl groups, 2-propanol was observed to remain molecularly adsorbed on the Co_3O_4(001) surface and where complete deactivation of the surface oxygen was observed.[10]

4. Experimental Section

Vibrational sum frequency spectroscopy is a second-order nonlinear optical process, the details of which are elucidated by Y.R Shen and several other authors.[25–28] In brief, sum frequency was generated when an IR light wave was mixed with a visible light beam at the interface. As it is second-order process it only carries information from the interfacial region. Moreover, this process is particularly useful if the IR wavelength matches a vibrational resonance in the adlayer such that tuning the IR light allows us to obtain the vibration spectrum. In our experiment, a scanning vSF spectrometer with ≈12 cm^{-1} resolution was used (Ekspla PL2231 and PG501DFG) that utilized wavelength tunable IR pulses of 25 ps duration and 532 nm light pulses for upconversion at a repetition rate of 50 Hz. Pulse energies of 280 μJ (532 nm) and 10–30 μJ (IR) were applied. For every data point, typically 400 laser pulses were sampled and averaged. In order to normalize the data with respect to day-to-day fluctuations in laser performance, the reference signal from an Au sample was used.

The experimental setup was previously described in detail in our published work.[10,13,14] The samples were mounted in a home-built compact cell (63 mm inner diameter) that allowed for the preservation of a rough vacuum before admitting 50 mbar of 2-propanol utilizing an evaporator to obtain a nearly saturated alcohol atmosphere above the substrate surface. The laser beams entered, and the signal left the cell through a MgF_2 window. The IR and upconversion light beams were directed at the sample under incident angles of 40° and 54° with respect to the surface normal, respectively. Before recording any spectra, the samples were further cleaned utilizing a two-stage cleaning process: 1) exposure to an oxygen plasma (0.4 mbar, 15–30 min) and 2) in situ exposure to UV irradiation from a Xe lamp (Osram, XBO 150 W/1) in the presence of an oxygen atmosphere (100–200 mbar, 2–5 h). Alcohol was flown from a temperature-controlled reservoir through the reaction cell, which was evaporated by the vacuum pump. Anhydrous 2-propanol (99.5%) was obtained from Sigma-Aldrich and used without further purification.

The spectra were fit using the following established expression[29,30]

$$I^{SFS}(\omega_{IR}) \propto \left| |\chi^{(2)}_{NR}| + \sum_i e^{i\xi} \frac{A_i}{\omega_{IR} - \omega_i + i\Gamma_i} \right|^2 \quad (1)$$

where $\chi^{(2)}_{NR}$ represents the second-order susceptibility of the substrate electronic system leading to a nonresonant background. A_i, ω_i, and Γ_i are the VSF line strength, the position, and the width (HWHM) of the i^{th} vibrational resonance, respectively. ω_{IR} is the angular frequency of the incident IR light.

The surface density of an adsorbed species N_s could be inferred from the A_i values derived from the fit to a spectrum as they were connected according to the following expression[31]

$$A_i = N_s < a_i >_f = N_s \int a_i f(\Omega) d \quad (2)$$

where N_s is the surface density of molecules, a_i is the nonlinear molecular hyperpolarizability strength associated with the i^{th} vibrational resonance, $< >_f$ indicates an average with respect to the orientational distribution function f (Ω), and Ω denotes the set of three Euler angles.

Acknowledgements

This research was funded by the Deutsche Forschungsgemeinschaft (DFG, German Research Foundation)—Project ID No. 388390466—CRC/TRR 247 "Heterogeneous Oxidation Catalysis in the Liquid Phase." S.K. acknowledges the computing time granted by the Center for Computational Sciences and Simulation (CCSS) of the University of Duisburg-Essen and provided on the supercomputer magnitUDE (DFG grants INST 20876/209-1 FUGG, INST 20876/243-1 FUGG) at the Zentrum für Informations-und Mediendienste (ZIM). A.B acknowledges the start-up grant UoH-IOE-SG-24-005 by the Institute of Eminence, University of Hyderabad, India.

Conflict of Interest

The author declares no conflict of interest.

Data Availability Statement

The data that support the findings of this study are available in the supplementary material of this article.

Keywords: alcohol adsorption · cobalt ferrite metal oxides · in situ vibrational sum frequency spectroscopy

[1] H. G. Yang, C. H. Sun, S. Z. Qiao, J. Zou, G. Liu, S. C. Smith, H. M. Cheng, G. Q. Lu, *Nature* **2008**, *453*, 638.
[2] M. Li, Z. Wu, S. H. Overbury, *J. Catal.* **2013**, *306*, 164.
[3] T. Tachikawa, S. Yamashita, T. Majima, *J. Am. Chem. Soc.* **2011**, *133*, 7197.
[4] Y.-K. Peng, S. C. E. Tsang, *Nano. Today* **2018**, *18*, 15.
[5] S. Najafishirtari, K. Friedel Ortega, M. Douthwaite, S. Pattisson, G. J. Hutchings, C. J. Bondue, K. Tschulik, D. Waffel, B. Peng, M. Deitermann, G. W. Busser, M. Muhler, M. Behrens, *Chem.Eur. J.* **2021**, *27*, 16809.
[6] L. Chen, J. Tang, L.-N. Song, P. Chen, J. He, C.-T. Au, S.-F. Yin, *Appl. Catal. B* **2019**, *242*, 379.
[7] T. Falk, E. Budiyanto, M. Dreyer, C. Pflieger, D. Waffel, J. Büker, C. Weidenthaler, K. F. Ortega, M. Behrens, H. Tüysüz, M. Muhler, B. Peng, *ChemCatChem* **2021**, *13*, 2942.

[8] T. Falk, E. Budiyanto, M. Dreyer, J. Büker, C. Weidenthaler, M. Behrens, H. Tüysüz, M. Muhler, B. Peng, *ACS Appl. Nano. Mater.* **2022**, *5*, 17783.
[9] A. H. Omranpoor, S. Kenmoe, *Catalysts* **2023**, *14*, 25.
[10] A. H. Omranpoor, A. Bera, D. Bullert, M. Linke, S. Salamon, S. Webers, H. Wende, E. Hasselbrink, E. Spohr, S. Kenmoe, *J. Chem. Phys.* **2023**, *158*, 164703.
[11] D. Yang, Y. Li, X. Liu, Y. Cao, Y. Gao, Y. R. Shen, W.-T. Liu, *Proc. Natl. Acad. Sci.* **2018**, *115*, E3888.
[12] A. Bera, D. Bullert, E. Hasselbrink, *J. Phys. Chem. C* **2020**, *124*, 16069.
[13] A. Bera, D. Bullert, M. Linke, E. Hasselbrink, *J. Phys. Chem. C* **2021**, *125*, 7721.
[14] A. Bera, D. Bullert, M. Linke, S. Franzka, U. Hagemann, N. Hartmann, E. Hasselbrink, *Catal. Sci. Technol.* **2023**, *13*, 4988.
[15] G. A. Somorjai, S. K. Beaumont, S. Alayoglu, *Angew. Chem., Int. Ed.* **2011**, *50*, 10116.
[16] G. A. Somorjai, G. Rupprechter, *J. Chem. Educ.* **1998**, *75*, 161.
[17] G. A. Somorjai, G. Rupprechter, *J. Phys. Chem. B* **1999**, *103*, 1623.
[18] H.-J. Freund, H. Kuhlenbeck, J. Libuda, G. Rupprechter, M. Bäumer, H. Hamann, *Top. Catal.* **2001**, *15*, 201.
[19] A. Holm, B. Davies, S. Boscolo Bibi, F. Moncada, J. Halldin-Stenlid, L. Paškevičius, V. Claman, A. Slabon, C.-W. Tai, E. Campos dos-Santos, S. Koroidov, *ACS Catal.* **2024**, *14*, 3191.
[20] P. Scheiber, M. Fidler, O. Dulub, M. Schmid, U. Diebold, W. Hou, U. Aschauer, A. Selloni, *Phys. Rev. Lett.* **2012**, *109*, 136103.
[21] A. H. Omranpoor, T. Kox, E. Spohr, S. Kenmoe, *Appl. Surf. Sci. Adv.* **2022**, *12*, 100319.
[22] D. H. Douma, K. N. Nono, A. H. Omranpoor, A. Lamperti, A. Debernardi, S. Kenmoe, *J. Phys. Chem. C* **2023**, *127*, 5351.
[23] T. Kox, A. H. Omranpoor, S. Kenmoe, *Physchem* **2022**, *2*, 321.
[24] T. Kox, S. Kenmoe, *Dalton Trans.* **2024**, *53*, 13184.
[25] Y. R. Shen, *Nature* **1989**, *337*, 519.
[26] C. S. Tian, Y. R. Shen, *Surf. Sci. Rep.* **2014**, *69*, 105.
[27] L. J. Richter, T. P. Petralli-Mallow, J. C. Stephenson, *Opt. Lett.* **1998**, *23*, 1594.
[28] A. G. Lambert, P. B. Davies, D. J. Neivandt, *Appl. Spectrosc. Rev.* **2005**, *40*, 103.
[29] M. Buck, M. Himmelhaus, *J. Vac. Sci. Technol., A* **2001**, *19*, 2717.
[30] F. Vidal, A. Tadjeddine, *Rep. Prog. Phys.* **2005**, *68*, 1095.
[31] X. Wei, X. Zhuang, S.-C. Hong, T. Goto, Y. R. Shen, *Phys. Rev. Lett.* **1999**, *82*, 4256.

Manuscript received: February 24, 2025
Revised manuscript received: June 16, 2025
Version of record online: August 11, 2025